

Probing the three-vector-boson vertex at hadron colliders

Dieter Zeppenfeld and Scott Willenbrock

Physics Department, University of Wisconsin, Madison, Wisconsin 53706

(Received 8 September 1987; revised manuscript received 5 February 1988)

Deviations of the ZWW vertex from the gauge theory prediction lead to an enhanced production of WZ boson pairs at large invariant masses at the CERN Large Hadron Collider (LHC) and the Superconducting Super Collider (SSC). The most general deviations observable in $q\bar{q}$ annihilation are parametrized in terms of seven form factors, whose high-energy behavior is severely restricted by unitarity. Even when taking these unitarity constraints into account, $W^\pm Z$ production at the LHC and SSC is up to 10 times more sensitive to anomalous ZWW couplings than W^+W^- production in e^+e^- annihilation at the CERN e^+e^- collider LEP II.

I. INTRODUCTION

Despite the success of the standard electroweak theory, there is to date no direct experimental evidence for the vector-boson self-interactions which are predicted by this model. These interactions are a manifestation of the non-Abelian gauge symmetry upon which the theory is based. The observation of these self-interactions is a stringent test of the theory.

In this paper we will study the ability of future high-energy hadron colliders to probe the three-vector-boson self-interactions. In particular, we will concentrate on probing the ZWW vertex via WZ -boson production from quark-antiquark annihilation.¹⁻⁵ The Feynman diagrams for this process are shown in Fig. 1. The ZWW vertex that we are interested in enters via the third diagram: s -channel exchange of a virtual W .

Most of the work which has been done on the topic of probing the vector-boson self-interactions has concentrated on the CERN LEP II electron-positron collider, which will be capable of pair-producing W bosons.⁶⁻⁸ Our goal is to compare the sensitivity to anomalous ZWW interactions of proposed pp colliders such as the CERN Large Hadron Collider (LHC) ($\sqrt{s} = 17$ TeV) and the Superconducting Super Collider (SSC) ($\sqrt{s} = 40$ TeV) with the LEP II e^+e^- collider.

The main advantage of future hadron colliders over LEP II is the much higher machine energy. LEP II will produce W -boson pairs just above threshold ($\sqrt{s} = 180-200$ GeV), whereas the LHC and the SSC will be capable of producing vector-boson pairs of much higher invariant masses. Anomalous vector-boson self-interactions leads to amplitudes which grow with energy, so deviations from the standard model are more apparent at higher vector-boson-pair invariant masses. It is for this reason that future hadron colliders may be more sensitive probes of the vector-boson self-interactions than LEP II.

Hadron colliders are capable of producing vector-boson pairs in both charged and neutral channels, whereas electron-positron colliders are restricted to the latter. We believe that the best channel for studying the ZWW interaction at hadron colliders is WZ boson pro-

duction (Fig. 1), rather than W -boson pair production.^{9,10} There are several reasons for this, which we list below.

(i) The WZ -boson final state is easier to observe than that of W -boson pairs. Leptonic decays of the vector bosons result in the loss of only one neutrino for WZ bosons, while two neutrinos are lost for W -boson pairs. The momentum of a single missing neutrino may be reconstructed (up to a twofold ambiguity) from the measurement of the missing transverse momentum. If two neutrinos are lost, however, it is impossible to reconstruct their momenta at hadron colliders; too much information is lost. One may consider hadronic decays of the W bosons or mixed hadronic-leptonic modes, but these are plagued by large QCD backgrounds.¹¹ The production of WZ bosons followed by leptonic decays of the vector bosons is essentially background-free.

(ii) The WZ -boson channel is much less likely to receive contributions from new physics other than anomalous vector-boson self-interactions than the W -boson-pair channel. The latter may receive contributions from the Higgs boson (via WW scattering or gluon fusion), a new Z' boson, or new, heavy fermions which are pair produced and decay to real W bosons. The most likely new particle to contribute to the WZ -boson channel is a new W' boson. However, there are many models, including the currently popular E_6 models motivated by superstrings, which have a new Z' boson but no new W' boson at low energies. It is also possible that a charged Higgs

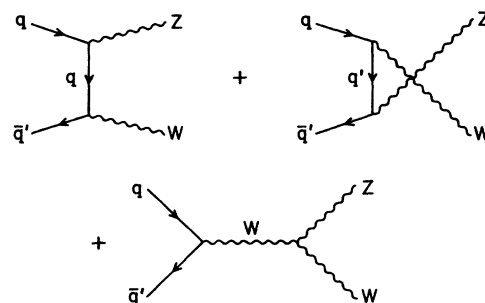


FIG. 1. Feynman graphs contributing to WZ production in hadron-hadron collisions.

boson could contribute to the WZ -boson channel. However, in models containing only Higgs doublets, this possibility is excluded because there is no tree-level WZH coupling.¹²

(iii) The WZ -boson channel allows one to study the ZWW vertex alone, while W -boson pair production is influenced by both the ZWW and γWW vertices. While W -boson pair production probes a larger set of vector-boson self-interactions, it is difficult to disentangle the photon and Z -boson contributions to the W -pair cross section.

(iv) The WZ -boson channel is more sensitive to certain three-vector-boson self-interactions than the W -boson-pair channel, and conversely, less sensitive to others. In this sense it provides information on the ZWW vertex which is complementary to that of W -boson pairs. (This point will be discussed in detail in Sec. IV.)

One may be concerned that in the presence of anomalous vector-boson self-interactions, the dominant source of WZ bosons may be WZ scattering rather than quark-antiquark annihilation. Although WZ scattering is higher order in the (weak) coupling of the vector bosons to fermions, it seems possible that the non-standard four-vector-boson self-interaction could be much stronger than the three-vector-boson self-interaction. For example, if the Higgs-boson mass is about 1 TeV, then the WZ scattering cross section is comparable to the cross section for WZ -boson production from quark-antiquark annihilation, in the standard model.¹³ This represents a scenario in which the three-vector-boson interaction is given by the standard model but the four-vector-boson vertex function is almost maximal, since the $J=0$ partial-wave amplitude for WZ scattering saturates the unitarity bound. This scenario is unlikely in more general models of anomalous vector-boson self-interactions. As we shall see, anomalous three-vector-boson self-interactions result in a large increase of the cross section (as compared to the standard-model prediction) for WZ -boson production from quark-antiquark annihilation. Therefore, in general, WZ scattering will not be a large background to the observation of anomalous three-vector-boson self-

interactions.

Another source of vector bosons which could potentially provide a large background to WZ -boson pair production is vector-boson bremsstrahlung off light quarks.¹⁴ However, it is easy to eliminate this background by imposing rapidity cuts on the vector bosons or their decay products, which we will do in the subsequent calculations.

We shall assume throughout that the vector-boson interactions with fermions are just those prescribed by the standard model. We certainly know experimentally that this is true with good accuracy at low energies, so any nonstandard interactions are necessarily small, and we shall neglect them.

The remainder of this paper is organized as follows. In Sec. II we write down the most general ZWW vertex and use it to derive the seven nontrivial helicity amplitudes for the process $q\bar{q} \rightarrow WZ$ in the high-energy limit. In Sec. III we discuss the unitarity bounds on the form-factors associated with the ZWW vertex. Section IV is devoted to presenting and discussing our numerical results for WZ -boson production at the LHC and the SSC. Finally, in Sec. V we compare the ability of the LHC and the SSC with that of LEP II to probe the ZWW vertex. Analytic formulas for the complete production and decay process $q\bar{q} \rightarrow WZ \rightarrow 4$ fermions are given in an Appendix.

II. THE ZWW VERTEX

The production of WZ -bosons from quark-antiquark annihilation involves the ZWW vertex via the s -channel exchange of a W boson, as shown in Fig. 1. In order to study deviations from the standard model, we must employ a general ZWW vertex. The most general ZWW coupling consistent with Lorentz invariance may be parametrized in terms of seven form factors, if we exclude terms proportional to $\partial_\mu W^\mu$ and $\partial_\mu Z^\mu$. These terms vanish if the vector bosons are coupled to massless fermions, which, to a good approximation, is the case in the process we are considering. Following Ref. 7 we write the effective Lagrangian

$$\begin{aligned}
 -\mathcal{L}_{WZ} / e \cot\theta_W = & ig_1 (W_{\mu\nu}^\dagger W^\mu Z^\nu - W_\mu^\dagger Z_\nu W^{\mu\nu}) + i\kappa W_\mu^\dagger W_\nu Z^{\mu\nu} + \frac{i\lambda}{M_W^2} W_{\lambda\mu}^\dagger W^\mu Z^{\nu\lambda} - g_4 W_\mu^\dagger W_\nu (\partial^\mu Z^\nu + \partial^\nu Z^\mu) \\
 & + g_5 \epsilon^{\mu\nu\rho\sigma} (W_\mu^\dagger \tilde{\partial}_\rho W_\nu) Z_\sigma + i\tilde{\kappa} W_\mu^\dagger W_\nu \tilde{Z}^{\mu\nu} + \frac{i\tilde{\lambda}}{M_W^2} W_{\lambda\mu}^\dagger W^\mu \tilde{Z}^{\nu\lambda}, \quad (2.1)
 \end{aligned}$$

where Z^μ and W^μ are the Z and W^- fields, respectively, $W_{\mu\nu} = \partial_\mu W_\nu - \partial_\nu W_\mu$, $Z_{\mu\nu} = \partial_\mu Z_\nu - \partial_\nu Z_\mu$, $\tilde{Z}_{\mu\nu} = \frac{1}{2}\epsilon_{\mu\nu\rho\sigma} Z^{\rho\sigma}$, and $(A \tilde{\partial}_\mu B) = A(\partial_\mu B) - (\partial_\mu A)B$. There are five dimension-four operators, and two of dimension six. We have scaled the latter with respect to M_W^2 , following the convention used in Refs. 6 and 7.

The couplings g_1 , κ , and λ respect the discrete symmetries C and P . In the standard model, at the tree level, $g_1 = 1$, $\kappa = 1$, and $\lambda = 0$. The coupling g_4 respects P but is odd under C . The couplings g_5 , $\tilde{\kappa}$, and $\tilde{\lambda}$ are P odd, and the former is also C odd, while the latter two are C even. In the standard model, the couplings which violate C or P are of order α or higher.

From the Lagrangian (2.1) we may derive a momentum-space vertex as shown in Fig. 2. Again following Ref. 7 we write

$$\begin{aligned}
 \Gamma^{\alpha\beta\mu}(q, \bar{q}, P) = & f_1 Q^\mu g^{\alpha\beta} - \frac{f_2}{M_W^2} Q^\mu P^\alpha P^\beta + f_3 (P^\alpha g^{\mu\beta} - P^\beta g^{\mu\alpha}) + i f_4 (P^\alpha g^{\mu\beta} + P^\beta g^{\mu\alpha}) + i f_5 \epsilon^{\mu\alpha\beta\rho} Q_\rho \\
 & - f_6 \epsilon^{\mu\alpha\beta\rho} P_\rho - \frac{f_7}{M_W^2} Q^\mu \epsilon^{\alpha\beta\rho\sigma} P_\rho Q_\sigma, \quad (2.2)
 \end{aligned}$$

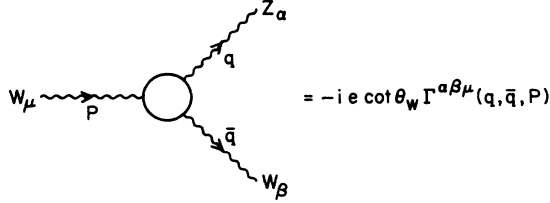


FIG. 2. Feynman rule for the general ZWW vertex. The vertex function Γ is given in Eq. (2.2).

where $Q = q - \bar{q}$ and $P = q + \bar{q}$. The seven form factors f_i are dimensionless functions of q^2 , \bar{q}^2 , and $P^2 = s$. For the production of $W^\pm Z$, with on-shell vector bosons, i.e., $q^2 = m_Z^2$, $\bar{q}^2 = m_W^2$, we denote the form factors by f_i^\pm . They are related to the coupling constants in the effective Lagrangian (2.1) by

$$\begin{aligned}
 f_1^\pm &= \mp \frac{1}{2} \left[g_1 + \kappa + \frac{s}{M_W^2} \lambda \pm i g_4 \right], \\
 f_2^\pm &= \mp \lambda, \\
 f_3^\pm &= \mp \frac{1}{2} \left[3g_1 + \kappa + \frac{M_Z^2 + M_W^2}{M_W^2} \lambda \mp i g_4 \right], \\
 i f_4^\pm &= \mp \frac{1}{2} \left[g_1 - \kappa + \frac{M_Z^2 - M_W^2}{M_W^2} \lambda \pm i g_4 \right], \\
 i f_5^\pm &= \mp \frac{1}{2} \left[\bar{\kappa} \pm i g_5 - \frac{M_Z^2 - M_W^2}{M_W^2} \bar{\lambda} \right], \\
 f_6^\pm &= \pm \frac{1}{2} \left[\bar{\kappa} \mp 3i g_5 + \frac{M_Z^2 + M_W^2}{M_W^2} \bar{\lambda} \right], \\
 f_7^\pm &= \pm \frac{1}{2} \bar{\lambda}.
 \end{aligned} \tag{2.3}$$

We have calculated the cross section for WZ -boson production followed by leptonic decay using the formalism developed in Refs. 7 and 15. This method is exact (at the tree level), including spin correlations and finite-width effects of the vector bosons. The details of the calculation are described in the Appendix.

For a qualitative discussion of the effects of anomalous contributions to the ZWW vertex, it is convenient to study the high-energy behavior of the helicity amplitudes $\mathcal{M}(\sigma_1 \sigma_2; \lambda_1 \lambda_2)$ for the parton subprocess $q(\sigma_1) + \bar{q}(\sigma_2) \rightarrow Z(\lambda_1) + W^\pm(\lambda_2)$. Here σ_i and λ_i denote the helicities of the incoming quarks and the produced vector bosons, respectively. Separating some overall factors we write

$$\begin{aligned}
 \mathcal{M}(\sigma_1 \sigma_2; \lambda_1 \lambda_2) &= \pm e^2 \frac{\cos \theta_W}{\sin^2 \theta_W} \beta \frac{s}{s - M_W^2} \\
 &\quad \times \delta_{\sigma_1 - \delta_{\sigma_2}} A_{\lambda_1 \lambda_2}(\Theta) d_{-1, \lambda_1 - \lambda_2}^{J_0}(\Theta).
 \end{aligned} \tag{2.4}$$

Here Θ is the center-of-mass scattering angle of the Z with respect to the quark direction, $\beta = |\mathbf{q}| / (\sqrt{s}/2)$ in terms of the vector-boson three-momentum \mathbf{q} , and

$J_0 = \max(1, |\lambda_1 - \lambda_2|)$ is the minimum angular momentum of the WZ system. The dominant angular dependence has been separated in terms of the conventional d functions;¹⁶ however, the u - and t -channel poles of the first two graphs in Fig. 1 still imply a strong angular variation of the reduced amplitudes $A_{\lambda_1 \lambda_2}$.

Within the standard model, at fixed scattering angle Θ , gauge theory cancellations between the u -, t -, and s -channel exchange graphs of Fig. 1 render the reduced amplitudes bounded from above as the center-of-mass energy increases. This ceases to be true if any of the coupling constants in the effective Lagrangian (2.1) differ from their standard-model values. At high energies the anomalous contributions completely dominate the cross section and for a qualitative discussion it suffices to consider the high-energy limit of the deviations $\Delta A_{\lambda_1 \lambda_2}$ from the standard-model prediction, that are due to anomalies in the ZWW vertex. Furthermore, the W - Z mass difference is unimportant in this limit, i.e., $\Delta A_{\lambda_1 \lambda_2}$ can be written in terms of $\gamma \approx \sqrt{s}/2M_W \approx \sqrt{s}/2M_Z$.

This high-energy behavior is summarized in Table I for both W^+Z and W^-Z production. Also included are the d functions that multiply the reduced amplitudes A in Eq. (2.4). These results can be easily obtained from Eqs. (2.3) and the matrix elements for W^+W^- production in e^+e^- annihilation, as given in Ref. 7. Table I will be extensively used in the following.

III. FORM FACTORS AND UNITARITY

The anomalous couplings, which were introduced in the previous section via the effective Lagrangian (2.1), lead to deviations from the standard-model prediction for the amplitudes for WZ production. These deviations grow with energy, so the $J = 1$ partial-wave amplitude of the process $q\bar{q} \rightarrow WZ$, which is the only partial wave to which the ZWW vertex contributes, will eventually violate unitarity if constant anomalous couplings are assumed. This means that any anomalous coupling has to be introduced as a form factor which decreases at high invariant masses. Since multi-TeV hadron colliders cover a wide range of ZW invariant masses, this form-factor behavior should not be neglected in a realistic study.

Stringent unitarity bounds on the form factors corresponding to the various couplings in Eq. (2.1) can be obtained from the inelastic contributions to WZ and WW scattering. For WZ scattering, for example, consider the contribution from $WZ \rightarrow f_1 f_2$, where (f_1, f_2) generically denotes the two members of a fermionic $SU(2)_L$ doublet. Denoting the $J = 1$ inelastic partial-wave amplitude of $W^\pm Z \rightarrow l^\pm \nu$ by \mathcal{T}^i and the corresponding elastic amplitude for $W^\pm Z \rightarrow W^\pm Z$ by \mathcal{T}^e , unitarity of the S matrix implies

$$\text{Im } \mathcal{T}^e = |\mathcal{T}^e|^2 + (3+1)N |\mathcal{T}^i|^2 + \sum |\mathcal{T}^{\text{rest}}|^2. \tag{3.1}$$

Here $(3+1)N$ counts the leptons and 3 colors of quarks in $N = 3$ generations of light fermions, and $\mathcal{T}^{\text{rest}}$ denotes any additional inelastic contributions. Equation (3.1) is consistent only if

TABLE I. Deviations of the reduced amplitudes $A_{\lambda_Z \lambda_W}$ from their standard-model value due to anomalies in the ZWW vertex. Only leading terms in $\gamma \approx \sqrt{s}/2M_W \approx \sqrt{s}/2M_Z$ are given. The abbreviations $\Delta g_1 = g_1 - 1$ and $\Delta \kappa = \kappa - 1$ have been used. Also given are the d function that multiply the various $A_{\lambda_Z \lambda_W}$ in Eq. (2.4).

$(\lambda_Z \lambda_{W\pm})$	$\Delta A_{\lambda_Z \lambda_W}$	$d(\Theta)$
(+0)	$\gamma(\Delta g_1 + \Delta \kappa + \lambda \mp ig_4 - i\bar{\kappa} \mp g_5 - i\bar{\lambda})$	$\frac{1}{2}(1 - \cos\Theta)$
(0-)	$\gamma(2\Delta g_1 + \lambda \pm 2g_5 + i\bar{\lambda})$	$\frac{1}{2}(1 - \cos\Theta)$
(0+)	$\gamma(2\Delta g_1 + \lambda \mp 2g_5 - i\bar{\lambda})$	$\frac{1}{2}(1 + \cos\Theta)$
(-0)	$\gamma(\Delta g_1 + \Delta \kappa + \lambda \mp ig_4 + i\bar{\kappa} \pm g_5 + i\bar{\lambda})$	$\frac{1}{2}(1 + \cos\Theta)$
(++)	$2\gamma^2(\lambda - i\bar{\lambda})$	$\frac{1}{\sqrt{2}} \sin\Theta$
(--)	$2\gamma^2(\lambda + i\bar{\lambda})$	$\frac{1}{\sqrt{2}} \sin\Theta$
(00)	$2\gamma^2(\Delta g_1 \mp ig_4)$	$\frac{1}{\sqrt{2}} \sin\Theta$

$$4N |T^i|^2 \leq \frac{1}{4} \quad (3.2)$$

which is the desired unitarity bound. A more complete description will be given elsewhere.¹⁷

The results for WZ scattering at energies much larger than M_W and M_Z , assuming real form factors, can be summarized in terms of the inequality

$$|\Delta A_{\lambda_1 \lambda_2}| < \frac{6 \sin^2 \theta_W}{\alpha \cos \theta_W} \frac{1}{\sqrt{4N}} \approx 58 \quad (3.3)$$

for the reduced matrix element of Table I. The numerical value is obtained using $\sin^2 \theta_W = 0.23$, $\alpha = \alpha(M_W^2) \approx 1/128$, and $N = 3$ generations of fermions with universal couplings to W and Z bosons. The unitarity bound effectively limits the deviations ΔA from the standard model (SM) only, because the SM contribution to the $J = 1$ partial-wave amplitude is much smaller than the unitarity bound at all energies and may safely be neglected.

Using the expressions for the $\Delta A_{\lambda_1 \lambda_2}$ in terms of the anomalous ZWW couplings given in Table I, one obtains the maximal deviations of the ZWW vertex compatible with unitarity for any given WZ invariant mass $\sqrt{\hat{s}}$. Assuming that only one anomalous coupling deviates from its standard-model value, the bounds derived from Eq. (3.3) are

$$\gamma^2 |g_1 - 1| < 29, \quad (3.4a)$$

$$\gamma |\kappa - 1| < 58, \quad (3.4b)$$

$$\gamma^2 |\lambda| < 29, \quad (3.4c)$$

$$\gamma^2 |g_4| < 29, \quad (3.4d)$$

$$\gamma |g_5| < 29, \quad (3.4e)$$

$$\gamma |\bar{\kappa}| < 58, \quad (3.4f)$$

$$\gamma^2 |\bar{\lambda}| < 29, \quad (3.4g)$$

where $\gamma^2 \approx \hat{s}/4M_W^2 \approx \hat{s}/4M_Z^2$.

The above derivation of the bounds (3.4) assumes that the coupling of the W and Z bosons to the known quarks

and leptons is given by the standard-model value at all momentum transfers. We will always make this assumption in this paper; i.e., we only consider deviations from the SM which occur in the weak-boson sector. One may argue that stronger bounds can be derived from $WZ \rightarrow WZ$ elastic unitarity, because no weak fermion-boson-vertex enters in this case. However, elastic unitarity for WZ scattering will only limit combinations of three- and four-vector boson vertices and the bounds are hence not immediately useful for WZ production in fermion-antifermion annihilation.

The bounds of Eq. (3.4) imply that any anomalous three-boson couplings must be form factors which vanish at high energies. For $\lambda = 0.2$, for example, a value which will produce barely observable deviations from SM expectations at LEP II (Refs. 7 and 8) form factor effects must set in below $\sqrt{\hat{s}} = 2$ TeV in order to avoid a violation of unitarity. Since invariant masses of this size are easily produced at both the LHC and the SSC, the measurement of the ZWW vertex at multi-TeV hadron colliders cannot adequately be discussed without taking the form-factor behavior of anomalous couplings into account.

Throughout this paper we parametrize the form factor corresponding to some anomalous coupling c by

$$c = c(\hat{s}) = \frac{c_0}{(1 + \hat{s}/\Lambda^2)^n}, \quad (3.5)$$

usually choosing the minimal value for n compatible with unitarity. The actual functional form of $c(\hat{s})$ is of no particular importance, as long as a function monotonically decreasing with \hat{s} is chosen. The scale Λ in Eq. (3.5) corresponds to the energy where novel strong interactions in the weak-boson sector become important. At this scale one might also expect new resonances in WZ or WW scattering as well as in vector-boson pair production from fermion-antifermion annihilation.

We shall not discuss the observability of any resonance structure at $M \approx \Lambda$ in this paper. However, we shall always choose parameters for the form factors (3.5) such as to allow for an additional increase in the total cross section, due to resonances in the vicinity of $\sqrt{\hat{s}} = \Lambda$, without conflicting with unitarity. We thus investigate

the sensitivity of the LHC and the SSC to new physics in the weak-boson sector which manifests itself in almost-constant anomalous couplings at low energies plus resonances at the scale Λ , but without taking into account the improvement in sensitivity due to the latter. The bounds that we obtain will thus be conservative.

The room for additional resonance structure is demonstrated in Fig. 3, where $d\sigma(pp \rightarrow W^+Z+X, W^+ \rightarrow e^+/\mu^+\nu, Z \rightarrow e^+e^-/\mu^+\mu^-)/dM$ ($M = \sqrt{\hat{s}}$ is the WZ invariant mass) is plotted for three different cases: (i) the standard-model expectation (solid line), (ii) $\lambda = \lambda(\hat{s}) = 0.1/[1 + \hat{s}/(2 \text{ TeV})^2]$, with no other anomalous couplings (dotted line), and (iii) the unitarity bound for the complete $J=1$ partial wave (all helicity combinations of W and Z) in $u\bar{d} \rightarrow W^+Z$ (dashed line). This bound, derived from inelastic unitarity in $u\bar{d}$ scattering, is given by

$$\sigma(u\bar{d} \rightarrow W^+Z; \hat{s}; J=1) < \frac{\pi}{3\hat{s}}, \quad (3.6)$$

assuming that only left-handed quarks couple to the W boson, as in the standard model. The cross section bound (3.6) is slightly stronger than the corresponding bound implied by Eq. (3.3). Unitarity allows additional vector-boson resonances on top of the dotted line, as long as the resonance curve stays below the unitarity bound everywhere.

Assuming almost-constant form factors at low energy, as in Eq. (3.5), a more stringent bound on an anomalous value of κ is actually implied by unitarity in WW scattering. In terms of the momenta as defined for the vertex function $\Gamma^{\alpha\beta\mu}(q, \bar{q}, P)$ in Fig. 2, W^+W^- production

probes the form factor

$$c(\hat{s}) = c(q^2 = \hat{s}, \bar{q}^2 = M_W^2, P^2 = M_W^2) \quad (3.7a)$$

while ZW^+ production probes

$$c(\hat{s}) = c(q^2 = M_Z^2, \bar{q}^2 = M_W^2, P^2 = \hat{s}). \quad (3.7b)$$

At low-momentum transfer, $\hat{s} \ll \Lambda^2$, the two should coincide, however, and hence one has to satisfy the unitarity bound from W -boson pair production¹⁷

$$\frac{\hat{s}}{4M_W^2} |\kappa(q^2 = \hat{s}, \bar{q}^2 = M_W^2, P^2 = M_W^2) - 1| \lesssim 30, \quad (3.8)$$

which implies that κ falls at least as $1/\hat{s}$ asymptotically. For a fixed value of Λ this leads to a much more stringent bound on κ_0 , the low-energy value of κ , than Eq. (3.4b). In the following, this more stringent bound on κ will always be used.

Finally, let us remark on contributions to the anomalous couplings from radiative corrections within the standard model. The low-energy values of $\kappa-1$ and λ in the $WW\gamma$ vertex, for example, have been calculated by several authors,¹⁸ and values of the order of 0.01 are found. When comparing these values with the sensitivity of hadron colliders, to be discussed below, one must always keep in mind the momentum scale at which the couplings are measured. Deviations from $\kappa=1$ or $\lambda=0$ of only a few percent are measurable at the LHC or the SSC provided they remain almost constant up to energies where they cause the WZ cross sections to approach the unitarity bound, which should be expected if new strong interactions become operative in the weak-boson sector. In the standard model, however, the form factors vary on the scale given by the masses of particles in the loop diagrams, e.g., the weak-boson masses or heavy fermion masses, and the assumption of constant form factors will in general not hold. Within the standard model, with a reasonably low value of the Higgs-boson mass, we expect cross sections to stay close to the tree-level value at all energies, and hence we do not expect that WZ -boson production at the LHC or the SSC can serve to check radiative corrections within the standard model.

IV. SIGNALS FOR ANOMALOUS COUPLINGS

WZ -boson pairs will be copiously produced at the LHC and the SSC. The standard model predicts a total cross section of $\sigma_{\text{tot}}(pp \rightarrow W^\pm Z + X) \approx 95 \text{ pb}$ at $\sqrt{s} = 40 \text{ TeV}$. Of course only a small fraction of these events will be useful experimentally. Because it is uncertain whether weak-boson pairs can be identified when one of them decays hadronically,¹¹ we require both the W and the Z bosons to decay leptonically, more precisely into electrons or muons. For all three charged leptons we will impose a rapidity cut $|y| < 2.5$. These requirements reduce the signal to a few tenths of a pb, which still corresponds to several thousand events per year at a luminosity of $10^{33} \text{ cm}^{-2}\text{sec}^{-1}$. The standard-model values of cross sections, with and without cuts, are summarized in Table II.

The signal that we investigate thus consists of three isolated, energetic electrons or muons, with low hadronic

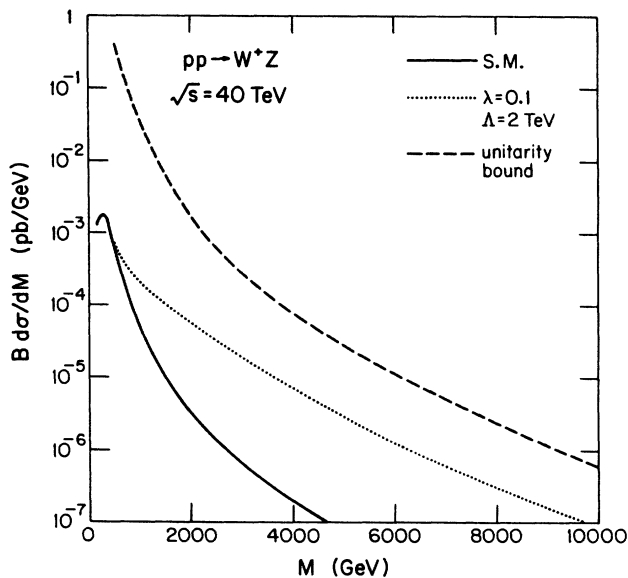


FIG. 3. Comparison of the standard model (solid line) and an anomalous coupling $\lambda(\hat{s}) = 0.1/[1 + \hat{s}/(2 \text{ TeV})^2]$ (dotted line) to the maximal cross section allowed by unitarity in the $J=1$ channel for the process $pp \rightarrow W^+Z, W^+ \rightarrow e^+/\mu^+\nu, Z \rightarrow e^+e^-/\mu^+\mu^-$. The quark distribution functions of Duke and Owens (set I) (Ref. 21) are used in this and all subsequent graphs. No rapidity cut is imposed on the decay leptons.

TABLE II. Standard-model values of WZ cross sections in pb. The combined branching fraction for both the W and the Z decaying into electrons and muons is $B = 1.2\%$. The rapidity cut applies to all charged leptons.

	$pp \rightarrow WZ, \sqrt{s} = 17 \text{ TeV}$		$pp \rightarrow WZ, \sqrt{s} = 40 \text{ TeV}$	
	W^+Z	W^-Z	W^+Z	W^-Z
σ_{tot}	18	13.5	54	40
$B\sigma_{\text{tot}}$	0.23	0.17	0.66	0.50
$B\sigma(y < 2.5)$	0.103	0.076	0.21	0.17

activity. The momenta of two opposite sign, same flavor leptons must reconstruct the Z -boson mass. This requirement should effectively eliminate any background from leptonic decays of heavy fermions. Events arising from WZ scattering or W and Z bremsstrahlung are not a serious background either, as discussed in the Introduction.

A few thousand clean leptonic decays of vector-boson pairs per year produced in proton-proton annihilation is almost identical to the rate expected at LEP II for the semileptonic decays of W^+W^- pairs.¹⁹ As far as statistics is concerned, a 200-GeV e^+e^- machine and a multi-TeV hadronic collider are thus comparable. Because of the higher WZ -boson invariant mass that can be produced at hadron colliders, these machines are considerably more sensitive to anomalies in the ZWW vertex, however. This fact is demonstrated in Figs. 4 and 5, where the W^+Z invariant-mass distribution for $\lambda=0.1$, $g_1=1.1$, $\kappa=0.5$, and $g_5=0.4$, at $\sqrt{s} = 17 \text{ TeV}$ and 40 TeV are compared to the standard-model expectation. Form factors as in Eq. (3.5) were chosen with $\Lambda=2 \text{ TeV}$, $n=1$ for Δg_1 and λ ; $\Lambda=2 \text{ TeV}$, $n=\frac{1}{2}$ for g_5 ; and $\Lambda=1.25 \text{ TeV}$, $n=1$ for $\Delta\kappa$. Except for $\Delta\kappa$, which is considerably larger, the couplings were chosen at or slightly below the observability limits at LEP II. At the SSC and, to a lesser extent, the LHC, they would produce clearly observable enhancements in the counting rate at high WZ invariant masses.

The one exception to the above conclusion is κ , for which the sensitivity in WZ -boson production is rather poor. This fact can be understood from Table I. The amplitudes for $q\bar{q} \rightarrow WZ$ grow at most as $\gamma\Delta\kappa$ while a deviation of g_1 from its standard-model value of unity produces an increase in A_{00} proportional to $\gamma^2\Delta g_1$. The role of Δg_1 and $\Delta\kappa$ is interchanged in W^+W^- production, which means that W^+W^- production at high invariant masses is more sensitive to $\Delta\kappa \neq 0$ while WZ -boson production should be studied to search for anomalous contributions to g_1 .

The invariant mass of the WZ -boson system is not directly observable experimentally, because of the momentum carried away by the neutrino arising from W decay. However, the complete neutrino momentum can be reconstructed, albeit with a twofold ambiguity. The transverse momentum of the neutrino is identified with the missing transverse momentum (\not{p}_T) of the event. Using the kinematical constraint that the neutrino and the third charged lepton should have an invariant mass close to M_W , one can then reconstruct the missing longitudinal neutrino momentum and hence the WZ -boson invariant

mass M , with a twofold ambiguity.^{11,20} Fortunately the two solutions for M are usually not too different, and a fairly reliable reconstruction of $d\sigma/dM$ is thus possible. The curves shown in Figs. 4 and 5 were obtained using this reconstruction procedure. Every event produces two entries in the $d\sigma/dM$ distribution. Also included in Figs. 4 and 5 is the "true" invariant-mass distribution $d\sigma/dM$ for the standard model (dashed-double-dotted line). For all the anomalous couplings shown in these two figures (except $\kappa=0.5$) the "true" and the reconstructed mass distributions are practically indistinguishable. The SM curve suffers most from the ambiguity problem because it is the steepest. This means that for very small deviations from the SM reconstruction errors in $d\sigma/dM$ have to be taken into account.

A very interesting distribution which is unaffected by the mass reconstruction is the transverse-momentum spectrum of the Z boson, $d\sigma/dp_{TZ}$. In the standard model most of the WZ -boson events cluster in the forward and backward region (in the WZ -boson rest frame) due to the t - and u -channel quark-exchange graphs of Fig. 1, and hence tend to produce Z bosons at low p_T .

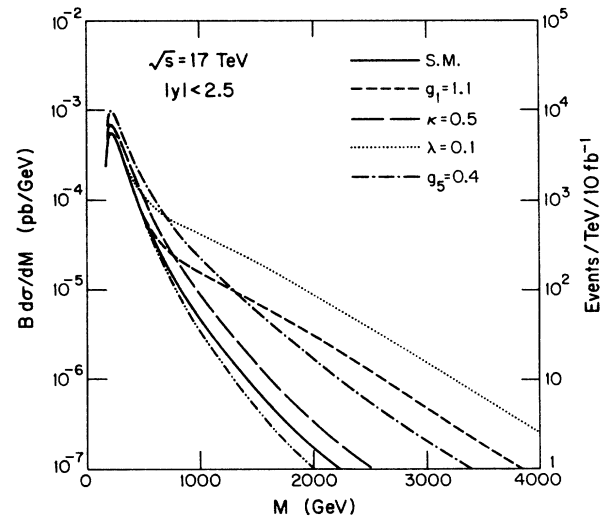


FIG. 4. Reconstructed WZ invariant-mass distribution in $pp \rightarrow W^+Z, W^+ \rightarrow l^+\nu, Z \rightarrow l'^+l'^-$ ($l, l' = e, \mu$) at the LHC for the standard model (solid line), $g_1=1.1$ (short-dashed line), $\lambda=0.1$ (dotted line), $g_5=0.4$ (dashed-dotted line), and $\kappa=0.5$ (long-dashed line). The true invariant-mass distribution (no twofold reconstruction ambiguity) is given for the standard model in addition (dashed-double-dotted line).

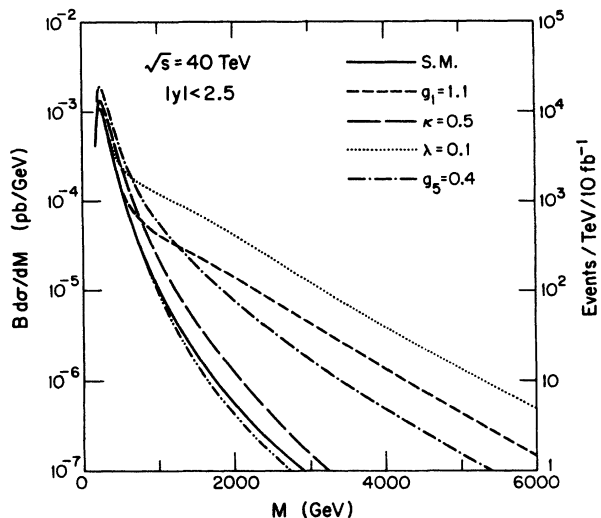


FIG. 5. Same as Fig. 4 but for the SSC. The scale on the right gives the number of events per TeV expected after one year of running.

However, the anomalous effects that we consider contribute to the $J=1$ partial wave only and thus lead to deviations from the standard-model angular distribution which are considerably more isotropic in the WZ -boson rest frame. As a result ZWW anomalous couplings favor the production of vector bosons at high p_T .

The effects of the ZWW couplings chosen in Figs. 4 and 5 on $d\sigma(pp \rightarrow W^+Z)/dp_{TZ}$ are shown in Figs. 6 and 7: all except anomalous values of κ lead to a large increase in event rate at high p_{TZ} . The p_T spectrum of the Z boson is at least as good an indicator of anomalous couplings as the invariant-mass distribution. Perhaps as importantly, the p_T of the Z may serve as a convenient

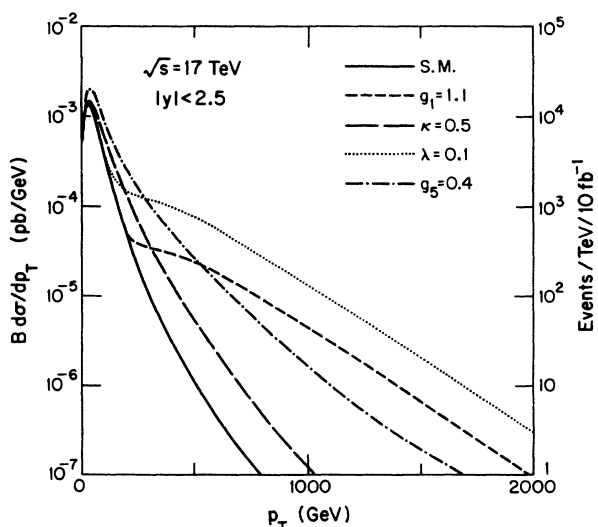


FIG. 6. Transverse-momentum spectrum of the Z boson in $pp \rightarrow W^+Z$ at the LHC. Distributions are given for the same couplings as in Fig. 4. As before both the vector bosons are required to decay into electrons or muons with rapidity $|y| < 2.5$.

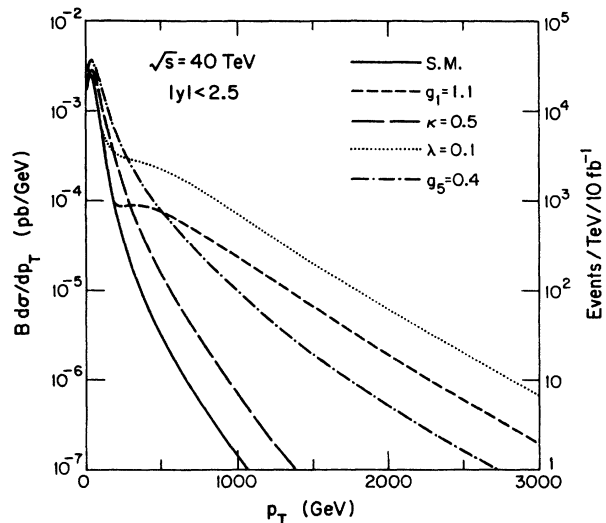


FIG. 7. Same as Fig. 6 but for the SSC ($\sqrt{s} = 40$ TeV).

cut to enhance the effects of new physics, e.g., when the decay distributions of the W and the Z boson are investigated.

The p_{TZ} and invariant-mass distributions may now be used to determine the sensitivity of the LHC and the SSC to anomalous contributions to the ZWW vertex. For this purpose we have chosen $n=2$ in the form factors of Eq. (3.5) for all anomalous couplings in order to avoid an excess of events with $M \gg \Lambda$, the scale of new interactions. As a criterion for observability we choose an excess of 50 W^+Z events (both vector bosons decaying into electron or muons) beyond the standard-model expectation in the regions $p_{TZ} > 250$ (220) GeV or $M > 800$ (600) GeV for an integrated luminosity of 10^{40} cm^{-2} at the SSC (LHC). The standard-model numbers are 40 (30) events and 70 (70) events in these two regions. In view of the fact that W^-Z events will enhance the statistics by a factor of 1.8 and a further increase is possible by the observation of τ decays of the W and Z bosons, our criterion is rather conservative.

The results of this sensitivity scan are given in Tables III and IV. Because of the form factors the sensitivity to the low-energy value of anomalous couplings increases with the scale of new physics Λ : a larger Λ implies a wider interval in M_{WZ} in which the cross section can be larger than in the standard model. Increasing Λ further, the unitarity bounds of Eqs. (3.4) and (3.8) finally get too stringent: unitarity forces the low-energy values of the form factor to be so small that no deviation from the standard model will be observable at the LHC nor at the SSC. This maximal observable scale is given by $\Lambda \approx 11-15$ TeV for the LHC and $\Lambda \approx 16-20$ TeV for the SSC. [Anomalous values of g_5 and $\bar{\kappa}$ formally allow one to probe scales up to $\Lambda \approx 100$ TeV, without violating the unitarity bounds (3.4). To have these two couplings which violate CP and/or P , close to their unitarity bound would leave a more restricted set of dynamical models, however.] Even though these values are somewhat uncertain (different assumptions on the form factors could lower them by as much as a factor 2), they considerably exceed the largest vector-boson-pair invariant masses

TABLE III. Minimal anomalous coupling c_0 observable at the LHC ($\sqrt{s} = 17$ TeV) for various form-factor scales Λ . A form factor $c(\hat{s}) = c_0 / (1 + \hat{s}/\Lambda^2)^2$ is assumed in all cases. The observability criterion is described in the text.

Λ (TeV)	1	2	3	5	9
Δg_1^0	+0.15	+0.07	+0.05	+0.04	+0.04
	-0.07	-0.03	-0.03	-0.025	-0.02
$\Delta \kappa^0$	+0.9	+0.5	+0.4		
	-0.5	-0.3	-0.3		
λ^0	± 0.07	± 0.04	± 0.03	± 0.025	± 0.02
g_4^0	± 0.11	± 0.06	± 0.05	± 0.04	± 0.03
g_5^0	± 0.35	± 0.20	± 0.15	± 0.14	± 0.12
$\bar{\kappa}^0$	± 0.75	± 0.45	± 0.35	± 0.3	± 0.3
$\bar{\lambda}^0$	± 0.07	± 0.035	± 0.025	± 0.02	± 0.018

that can be produced at these two hadron colliders. This opens the interesting possibility that both the LHC and the SSC may discover new physics in the weak-boson sector by finding small deviations from the gauge theory value of the ZWW vertex at energies considerably below the scale of new dynamics. Conversely, if no deviation in the p_T spectrum or in $d\sigma/dM$ is found and in particular if no resonances are seen in the latter, these machines can confirm the gauge theory values of g_1 , λ , g_5 , and $\bar{\lambda}$ at the 1–2 % level, an order of magnitude better than what can be achieved at LEP II.

The p_{TZ} and invariant-mass distributions will reveal the existence of anomalous couplings, if they are sufficiently large. However, in order to identify deviations in these spectra as anomalous ZWW couplings, one needs to study the angular distribution of the W or Z boson and of their decay products. The point is that these angular distributions allow, at least in principle, a determination of the W - and Z -boson helicities and thus an identification of anomalies as occurring in specific helicity components of the $J = 1$ partial wave.

The angular distributions of the WZ bosons and of their decay products are simplest in the center-of-mass frame and in the rest frames of the individual vector bosons in the case of decays. Since the WZ -boson invariant mass can be reconstructed experimentally, albeit with a twofold ambiguity, the angular distributions can approximately be reconstructed in their respective rest frames.

Figure 8 shows $d\sigma/d\cos\Theta$ at LHC energy, where $\cos\Theta$ is the scattering angle of the Z with respect to one of the proton beams in the reconstructed WZ rest frame.

Each event produces two entries in this figure, corresponding to the twofold ambiguity in the mass reconstruction. An $M > 600$ GeV cut was imposed in order to enhance the effect of anomalous couplings. Curves are shown for the standard model (solid line), $g_1 = 1.1$ (short dashed line) and $\lambda = 0.1$ (dotted line), both with $\Lambda = 2$ TeV, $n = 1$ in the form factor (3.5), $\kappa = 0.5$ (long dashed line) at $\Lambda = 1.25$ TeV and $n = 1$, and for $g_5 = 0.4$ (dashed-dotted line) at $\Lambda = 2$ TeV and $n = \frac{1}{2}$. The corresponding curves for the SSC are almost identical in shape. While the standard model curve is strongly peaked in the forward and backward directions, variations in g_1 and λ produce a $\sin^2\Theta$ distribution of the Z boson, as can be read off Table I: g_1 and λ produce the largest deviation in the reduced matrix elements A_{00} and $A_{\pm\pm}$, respectively. κ and g_5 , on the other hand, have their largest effect on the amplitudes $A_{\lambda_Z\lambda_W}$ with $|\Delta\lambda| = |\lambda_Z - \lambda_W| = 1$ and therefore produce a $1 + \cos^2\Theta$ distribution of the Z . Qualitatively, these different distributions are easily recognizable in Fig. 8.

Further information on the helicity combinations involved can be gained from the angular distributions of the decay products of the W and Z bosons. In Figs. 9 and 10 the $\cos\theta$ and $\cos\bar{\theta}$ distributions are shown for the same anomalous couplings and cuts as above. Here θ is the polar angle of the μ^- or e^- arising from Z decay with respect to the Z direction, and $\bar{\theta}$ is the polar angle of the e^+ or μ^+ from W^+ decay, again with respect to the Z direction. Both angles are determined in the rest frame of the respective vector boson. A reconstruction ambi-

TABLE IV. Same as Table III, but for $pp \rightarrow WZ$ at $\sqrt{s} = 40$ TeV (SSC).

Λ (TeV)	1	2	3	5	9
Δg_1^0	+0.14	+0.05	+0.04	+0.03	+0.02
	-0.05	-0.03	-0.015	-0.014	-0.010
$\Delta \kappa^0$	+0.7	+0.4	+0.3		
	-0.5	-0.3	-0.2		
λ^0	± 0.06	± 0.02	± 0.016	± 0.013	$\pm 9 \times 10^{-3}$
g_4^0	± 0.08	± 0.04	± 0.03	± 0.018	± 0.015
g_5^0	± 0.3	± 0.17	± 0.10	± 0.09	± 0.09
$\bar{\kappa}^0$	± 0.6	± 0.3	± 0.25	± 0.2	± 0.19
$\bar{\lambda}^0$	± 0.06	± 0.02	± 0.015	± 0.010	$\pm 9 \times 10^{-3}$

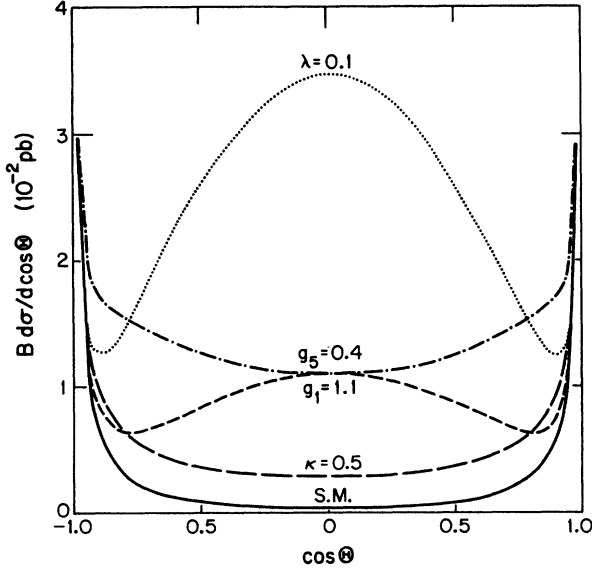


FIG. 8. Angular distribution of the Z boson in $pp \rightarrow W^+Z$ at $\sqrt{s} = 17$ TeV with respect to the beam axis. The scattering angle Θ is measured in the WZ rest frame. A cut $M_{WZ} > 600$ GeV is imposed on the WZ invariant mass. Anomalous couplings and form factors are chosen as in Fig. 4.

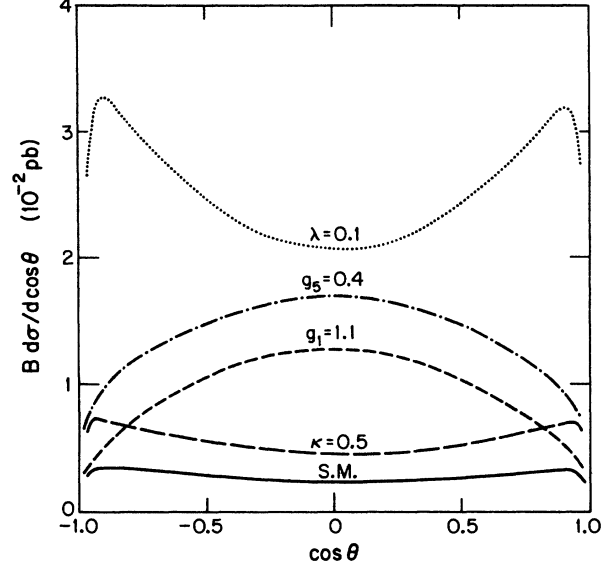


FIG. 9. Angular distribution of the negatively charged lepton in $pp \rightarrow ZW^+, Z \rightarrow l^+l^-$ at $\sqrt{s} = 17$ TeV. The lepton angle θ is measured in its parent's rest frame with respect to the Z momentum. Cuts and couplings are chosen as in Fig. 8.

guity arises only for the $\cos\bar{\theta}$ distribution.

Since the Z boson coupling to charged leptons is almost purely axial vector, both transverse polarizations $\lambda_Z = \pm 1$ produce a $\frac{1}{2}(1 + \cos^2\theta)$ distribution for the e^- or μ^- , while the angular distribution for longitudinal Z 's is $\sin^2\theta$. The corresponding distributions for the charged lepton arising from W^+ decay is $\frac{1}{2}(1 \mp \cos\theta)^2$ for $\lambda_W = \pm 1$ and $\sin^2\theta$ for $\lambda_W = 0$, the former being a direct consequence of the pure $V - A$ structure of the $\bar{f}fW$ couplings.

Keeping these distributions in mind one immediately recognizes from Figs. 9 and 10 that anomalous values of g_1 produce predominantly longitudinal Z 's and W 's, while $\lambda \neq 0$ results in a strong enhancement of transverse W 's and Z 's. More precisely, for $\lambda \neq 0$ the $\cos\theta$ distribution is nearly symmetric, implying the production of equal numbers of W 's with positive and negative helicity. Hence the decay-product polar-angle distributions resolve the ambiguity between λ and g_1 that remained from the study of the $\cos\Theta$ distribution of the Z alone. The above observations beautifully match with the expected behavior as implied by the $A_{\lambda_1\lambda_2}$ in Table I.

Once a deviation from the standard-model expectation is discovered in the p_T distribution of the Z or in $d\sigma/dM_{WZ}$, one may thus uniquely identify the source of the deviations, provided they arise from CP -nonviolating contributions to the ZWW vertex. CP -violating contributions (g_4 , $\bar{\kappa}$, and $\bar{\lambda}$) may be studied by comparing the W^+Z and W^-Z cross sections or by measuring azimuthal angle distributions and correlations of the decay products of the W and the Z . In order to perform an analysis of the angular distributions of the vector bosons and their decay products, a sufficiently large sample of excess WZ events is required, of course.

V. CONCLUSIONS

In this paper we have investigated the ability of the LHC and the SSC to measure the ZWW three-vector-boson vertex in WZ -boson production from $q\bar{q}$ annihilation. For the annihilation of light quarks any deviation from the standard model can be parametrized by seven anomalous couplings, three of which violate CP . As described in Sec. III, unitarity implies that all anomalous couplings must actually be form factors which vanish at asymptotic WZ invariant masses.

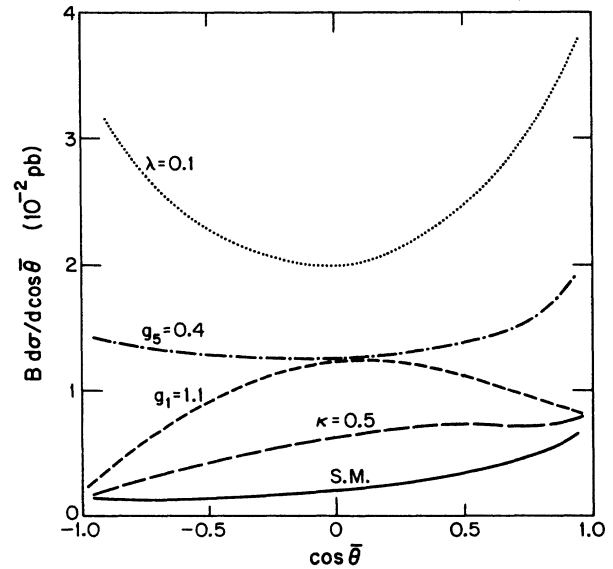


FIG. 10. Same as Fig. 9 but for the charged lepton in W^+ decay.

At LEP II the low-energy values of these form factors will be determined with a typical accuracy of 0.1–0.3 (depending on which coupling is assumed to deviate from the standard model)^{7,8} mainly by measuring the W angular distribution in the process $e^+e^- \rightarrow W^+W^-$, for which a clean event sample of a few thousand semileptonic decays is expected. A sample of roughly the same size (assuming a luminosity $\mathcal{L} = 10^{33} \text{ cm}^{-2}\text{sec}^{-1}$) is expected at LHC/SSC for $pp \rightarrow WZ$ with both vector bosons decaying into electrons and muons. Hence a statistical error comparable to the one at LEP is to be expected at LHC/SSC for the determination of the seven form factors at low invariant masses.

Since these two hadron colliders cannot be expected to do better than LEP in the determination of the form factors at low energies, we have concentrated on the measurement of the ZWW vertex at large WZ invariant masses M . Both the LHC and the SSC can produce WZ boson pairs with M in the TeV range. At masses of this order the rise of the parton cross section with increasing $\sqrt{\hat{s}} = M$, which is the result of deviations of the ZWW vertex from its standard-model form, starts to have dramatic effects even for very small values of the anomalous couplings. Assuming essentially constant form factors in the mass range $600 \text{ GeV} < \sqrt{\hat{s}} < 10 \text{ TeV}$, we find that values as small as 0.01–0.02 for anomalous couplings λ , Δg_1 , g_4 , or $\tilde{\lambda}$ will be clearly observable at LHC/SSC, the SSC usually being superior by a factor 2. Experiments at both hadron colliders would thus be one order of magnitude more sensitive to the ZWW vertex than experiments at LEP II.

A very strong constraint on deviations of the ZWW vertex from the gauge theory value is implied by the unitarity bounds discussed in Sec. III. If LEP II finds anomalous couplings $|\Delta g_1|$, $|\Delta \kappa|$, or $|\lambda| \approx 0.2$, these unitarity bounds imply that the dynamics producing the anomalous behavior of the ZWW vertex must occur at a scale $\Lambda < 2\text{--}3 \text{ TeV}$. If the scale is this low, LHC and SSC should be able to produce new resonances associated with the new interactions and do a detailed measurement of the various form factors in the ZWW vertex, as described in Sec. IV. If the scale Λ is larger than a few TeV, LEP II will certainly not see a deviation from the standard model while the SSC may observe first hints for new interactions in the weak-boson sector even if Λ is as large as 20 TeV. We thus find that the LHC and the SSC will be able to improve the measurement of the ZWW vertex, and thereby our knowledge of the weak boson sector, significantly beyond what is achievable at LEP II.

Note added in proof. The unitarity bounds of Eqs. (3.4) and (3.8) have been improved by up to a factor 1.6 in Ref. 17. Because of the margin allowed for additional resonance structure, the parameters used in the figures are still compatible with the more stringent unitarity requirements. Using the techniques described in Ref. 17 the cross-section bound of Eq. (3.6) can be improved by a factor of 4.

ACKNOWLEDGMENTS

This research was supported in part by the University of Wisconsin Research Committee with funds granted by

the Wisconsin Alumni Research Foundation, and in part by the U.S. Department of Energy under Contract No. DE-AC02-76ER00881.

APPENDIX

In Sec. II only the high-energy behavior of the WZ production amplitudes was considered. This high-energy behavior is sufficient to discuss the dominant effects of anomalous ZWW couplings in $pp \rightarrow WZ$. When these anomalous couplings are small, interference effects with the remaining standard-model amplitudes are important and a complete calculation of the differential cross section $d\sigma(pp \rightarrow WZ)$ is needed. In Sec. IV we have shown that the angular distributions of the W and the Z decay products are effective spin analyzers for the vector bosons and are of crucial importance when one tries to disentangle various sources for deviations in $d\sigma(pp \rightarrow WZ)$ from the SM expectation, in particular when trying to distinguish the various anomalous couplings in the effective Lagrangian (2.1) or, equivalently, the three-boson vertex (2.2).

What is needed, hence, are expressions for the complete differential cross section $d\sigma(pp \rightarrow WZ \rightarrow 4 \text{ fermions})$, or equivalently the corresponding partonic process, which includes all spin correlations between the vector bosons and their decay products. These expressions can be easily derived, and turned into a Monte Carlo program for event generation, by using amplitude calculation techniques. Here we use the helicity-amplitude formalism developed in Ref. 15 and our discussion closely parallels the one given in Ref. 7 for W^+W^- or ZZ production in e^+e^- annihilation.

In order to render this paper self-contained we first give a brief review of the helicity-amplitude calculus that we employ. We use the chiral representation of Dirac matrices for fermions and go to two-component notation. Spinors $\psi [=u(p, \lambda)]$ or $v(p, \lambda)$ are given by

$$\psi = \begin{bmatrix} \psi_- \\ \psi_+ \end{bmatrix}, \quad \bar{\psi} = (\psi_+^\dagger \quad \psi_-^\dagger), \quad (\text{A1})$$

with

$$u(p, \lambda)_\pm = \omega_{\pm\lambda}(p) \chi_\lambda(p), \quad (\text{A2})$$

$$v(p, \lambda)_\pm = \pm \lambda \omega_{\mp\lambda}(p) \chi_{-\lambda}(p).$$

Here λ denotes the helicity of the on-shell fermion with four-momentum $p^\mu = (E, p_x, p_y, p_z)$, $\chi_\lambda(p)$ is a normalized helicity eigenspinor, explicitly given by

$$\chi_+(p) = [2|\mathbf{p}|(|\mathbf{p}| + p_z)]^{-1/2} \begin{bmatrix} |\mathbf{p}| + p_z \\ p_x + ip_y \end{bmatrix}, \quad (\text{A3a})$$

$$\chi_-(p) = [2|\mathbf{p}|(|\mathbf{p}| + p_z)]^{-1/2} \begin{bmatrix} -p_x + ip_y \\ |\mathbf{p}| + p_z \end{bmatrix}, \quad (\text{A3b})$$

and

$$\omega_\pm(p) = (E \pm |\mathbf{p}|)^{1/2}. \quad (\text{A4})$$

Given the explicit form of γ matrices

$$\not{a} = a_\mu \gamma^\mu = \begin{pmatrix} 0 & \not{a}_+ \\ \not{a}_- & 0 \end{pmatrix}, \quad (\text{A5})$$

with

$$\not{a}_\pm = \begin{pmatrix} a^0 \mp a^3 & \mp (a^1 - ia^2) \\ \mp (a^1 + ia^2) & a^0 \pm a^3 \end{pmatrix}, \quad (\text{A6})$$

an arbitrary product of γ matrices with spinors at both ends can be expressed by the basic quantity

$$S(p_i, a_1, \dots, a_n, p_j)_{\lambda_i \lambda_j}^\alpha = \chi_{\lambda_i}^\dagger(p_i) (\not{a}_1)_\alpha (\not{a}_2)_{-\alpha} (\not{a}_3)_\alpha \cdots (\not{a}_n)_{\epsilon\alpha} \chi_{\lambda_j}(p_j) \quad (\text{A7})$$

for $\alpha = \pm$ [here $\epsilon = (-1)^{n-1}$]. Arbitrary polarization amplitudes are then expressed in terms of the basic quantity S , which is easily evaluated by 2×2 matrix multiplication.

The matrix elements for the process

$$\begin{aligned} u_i(k, \sigma) + \bar{d}_j(\bar{k}, \bar{\sigma}) &\rightarrow Z(q, \lambda) + W^+(\bar{q}, \bar{\lambda}), \\ Z(q, \lambda) &\rightarrow f_1(p_1, \sigma_1) \bar{f}_2(p_2, \sigma_2), \\ W^+(\bar{q}, \bar{\lambda}) &\rightarrow f_3(p_3, \sigma_3) \bar{f}_4(p_4, \sigma_4), \end{aligned} \quad (\text{A8})$$

will now be written in terms of the string of Pauli matrices S and the decay currents J_W^μ and J_Z^μ for W^+ and Z decay, to be given below. In Eq. (A8) i and j denote the colors of the u and \bar{d} quarks with helicities σ and $\bar{\sigma}$. λ and $\bar{\lambda}$ stand for the vector-boson helicities ($\lambda, \bar{\lambda} = \pm 1, 0$), $\sigma_1, \dots, \sigma_4$ are the helicities of the final-state leptons, and $k, \bar{k}, q, \bar{q}, p_1, \dots, p_4$ denote the four-momenta of the individual particles.

The complete amplitude for the process (A8) contains three terms corresponding to the t -, u -, and s -channel exchange graphs of Fig. 1:

$$\mathcal{M}(\sigma, \bar{\sigma}; \sigma_1, \sigma_2, \sigma_3, \sigma_4)_{ij} = \delta_{ij} (\mathcal{M}_t + \mathcal{M}_u + \mathcal{M}_s) \quad (\text{A9})$$

with

$$\begin{aligned} \mathcal{M}_t &= e^2 \frac{g_-^{Zuu} g_-^{Wud}}{(k-q)^2} \delta_{\sigma, -\delta_{\bar{\sigma}, +}} 2\sqrt{k^0 \bar{k}^0} D_Z(q^2) D_W(\bar{q}^2) \\ &\times S(\bar{k}, J_W, k-q, J_Z, k)_{--}, \end{aligned} \quad (\text{A10})$$

$$\begin{aligned} \mathcal{M}_u &= e^2 \frac{g_-^{Zdd} g_-^{Wud}}{(k-\bar{q})^2} \delta_{\sigma, -\delta_{\bar{\sigma}, +}} 2\sqrt{k^0 \bar{k}^0} D_Z(q^2) D_W(\bar{q}^2) \\ &\times S(\bar{k}, J_Z, k-\bar{q}, J_W, k)_{--}, \end{aligned} \quad (\text{A11})$$

and

$$\begin{aligned} \mathcal{M}_s &= e \frac{g_-^{Wud} g_{ZWW}}{s - M_W^2} \delta_{\sigma, -\delta_{\bar{\sigma}, +}} 2\sqrt{k^0 \bar{k}^0} D_Z(q^2) D_W(\bar{q}^2) \\ &\times S(\bar{k}, \Gamma, k)_{--}. \end{aligned} \quad (\text{A12})$$

The four vector Γ^μ is obtained from the vertex function $\Gamma^{\alpha\beta\mu}$ of Eq. (2.2) by contraction with the decay currents

$$\Gamma^\mu = \Gamma^{\alpha\beta\mu}(q, \bar{q}, P) J_{Z\alpha} J_{W\beta}, \quad (\text{A13})$$

the Z and W propagator factors $D_Z(q^2)$ and $D_W(\bar{q}^2)$ have the conventional Breit-Wigner form

$$D_V(q^2) = \frac{1}{q^2 - m_V^2 + im_V \Gamma_V} \quad (\text{A14})$$

and the ZWW coupling is given by

$$g_{ZWW} = -e \cot\theta_W. \quad (\text{A15})$$

The fermion couplings to the W and the Z are defined by the interaction Lagrangian

$$\mathcal{L}_{Vf_1f_2} = -e \sum_{\lambda=\pm} g_\lambda^{Vf_1f_2} \bar{\psi}_{f_1} \gamma_\mu P_\lambda \psi_{f_2} V^\mu, \quad (\text{A16})$$

where e denotes the positron charge and $P_\lambda = \frac{1}{2}(1 + \lambda\gamma_5)$ is the chiral projection matrix. The couplings we need are

$$\begin{aligned} g_+^{Zee} &= \tan\theta_W, \\ g_-^{Zee} &= -\frac{1}{2 \sin\theta_W \cos\theta_W} + \tan\theta_W, \\ g_-^{Zuu} &= \frac{1}{2 \sin\theta_W \cos\theta_W} - \frac{2}{3} \tan\theta_W, \\ g_-^{Zdd} &= -\frac{1}{2 \sin\theta_W \cos\theta_W} + \frac{1}{3} \tan\theta_W, \\ g_-^{Wf_1f_2} &= \frac{1}{\sqrt{2} \sin\theta_W}, \end{aligned} \quad (\text{A17})$$

where we neglect Cabibbo mixing for the quarks. The amplitudes for ZW^- production are obtained by interchanging u and d quarks in Eqs. (A8)–(A12). For the decays $Z \rightarrow f_1 \bar{f}_2$, $W^\pm \rightarrow f_3 \bar{f}_4$ (into massless fermions) the decay currents J_Z and J_W are given by

$$\begin{aligned} J_{Z\alpha}(\sigma_1, \sigma_2) &= -e g_{\sigma_1}^{Zf_1f_2} \delta_{\sigma_1, -\sigma_2} 2\sqrt{p_1^0 p_2^0} S(p_1, n^\alpha, p_2)_{\sigma_1 \sigma_1}^\alpha \quad (\text{A18}) \end{aligned}$$

and

$$\begin{aligned} J_{W\beta}(\sigma_3, \sigma_4) &= -e g_-^{Wf_3f_4} \delta_{\sigma_3, -\delta_{\sigma_4, +}} 2\sqrt{p_3^0 p_4^0} S(p_3, n^\beta, p_4)_{--}^\beta. \end{aligned} \quad (\text{A19})$$

Here n^μ is the unit vector in the μ direction; i.e., in the defining equation (A7) for the quantity S the Pauli matrix $(\sigma_\mu)_\pm$ enters instead of $(\not{a}_1)_\pm$. Equations (A18) and (A19) are valid for massless fermions. The generalization for massive fermions and decay matrix elements for $V \rightarrow q\bar{q}$ gluon can be found in Ref. 7. The differential cross section for the complete process (A8) is now given by

$$d\hat{\sigma} = \frac{1}{2s} \sum |\mathcal{M}|^2 d\phi_4, \quad (\text{A20})$$

where $d\phi_4$ is the invariant four-body phase-space

$$d\phi_4 = (2\pi)^4 \delta^4 \left[k + \bar{k} - \sum_{i=1}^4 p_i \right] \prod_{i=1}^4 \frac{d^3 p_i}{(2\pi)^3 2E_i}. \quad (\text{A21})$$

The color- and spin-averaged matrix element is

$$\sum |\mathcal{M}|^2 = \frac{1}{9} \sum_{i,j=1}^3 \frac{1}{4} \sum_{\sigma, \bar{\sigma}=\pm} \sum_{\sigma_1 \sigma_2 \sigma_3 \sigma_4=\pm} |\mathcal{M}(\sigma, \bar{\sigma}; \sigma_1, \sigma_2, \sigma_3, \sigma_4)_{ij}|^2 = \frac{1}{12} \sum_{\sigma_1=\pm} |\mathcal{M}_t + \mathcal{M}_u + \mathcal{M}_s|^2. \quad (\text{A22})$$

Here we have used the fact that $\mathcal{M}_{t,u,s}$ are proportional to $\delta_{\sigma, -\delta_{\bar{\sigma}, +}}$, that the decay current J_W contains the factor $\delta_{\sigma_3, -\delta_{\sigma_4, +}}$, and that J_Z is proportional to $\delta_{\sigma_1, -\sigma_2}$, when massless fermions are used in the calculation.

-
- ¹R. Brown, D. Sahdev, and K. Mikaelian, Phys. Rev. D **20**, 1164 (1979).
²C. Bilchak, R. Brown, and J. Stroughair, Phys. Rev. D **29**, 375 (1984).
³E. Eichten *et al.*, Rev. Mod. Phys. **56**, 579 (1984).
⁴G. Kane, in *Proceedings of the Summer Study on the Physics of the Superconducting Super Collider*, Snowmass, Colorado, 1986, edited by R. Donaldson and J. Marx (Division of Particles and Fields of the APS, New York, 1987), p. 7.
⁵M. Kuroda *et al.*, Nucl. Phys. **B284**, 271 (1987).
⁶K. Gaemers and G. Gounaris, Z. Phys. C **1**, 259 (1979).
⁷K. Hagiwara *et al.*, Nucl. Phys. **B282**, 253 (1987), and references therein.
⁸D. Zeppenfeld, Phys. Lett. B **183**, 380 (1987).
⁹C.-H. Chang and S.-C. Lee, Report No. FERMILAB-PUB-87/6-T, 1987 (unpublished); Phys. Rev. D **37**, 101 (1988); J. Stroughair and C. Bilchak, Z. Phys. C **23**, 377 (1984).
¹⁰M. Duncan, G. Kane, and W. Repko, Nucl. Phys. **B272**, 517 (1986).
¹¹J. Gunion, Z. Kunszt, and M. Soldate, Phys. Lett. **163B**, 389 (1985); J. Gunion and M. Soldate, Phys. Rev. D **34**, 826 (1986); W. Stirling *et al.*, Phys. Lett. **163B**, 261 (1985).
¹²J. Grifols and A. Mendez, Phys. Rev. D **22**, 1725 (1980).
¹³M. Chanowitz and M. Gaillard, Nucl. Phys. **B261**, 379 (1985).
¹⁴J. Gunion, J. Kalinowski, and A. Tofghi-Niaki, Phys. Rev. Lett. **57**, 2351 (1986).
¹⁵K. Hagiwara and D. Zeppenfeld, Nucl. Phys. **B274**, 1 (1986).
¹⁶Particle Data Group, M. Aguilar-Benitez *et al.*, Phys. Lett. **170B**, 1 (1986).
¹⁷U. Baur and D. Zeppenfeld, Phys. Lett. B (to be published).
¹⁸G. Couture *et al.*, Report No. TRI-PP-87-40, 1987 (unpublished) and references therein; T. Rizzo, Phys. Rev. D **32**, 43 (1985); J. Grifols, S. Peris, and J. Sola, Int. J. Mod. Phys. A **3**, 255 (1988); C. Bilchak and J. Stroughair, Bielefeld Report No. BI-TP-87/02, 1987 (unpublished); H. Neufeld, J. Stroughair and D. Schildknecht, Phys. Lett. B **198**, 563 (1987).
¹⁹G. Barbiellini *et al.*, in *Physics at LEP*, LEP Jamboree, Geneva, Switzerland, 1985, edited by J. Ellis and R. D. Peccei (CERN Report No. 86-02, Geneva, 1986), Vol. 2, p. 1; D. Treille *et al.*, in *Proceedings of the ECFA Workshop on LEP200*, Aachen, West Germany, 1986, edited by A. Böhm and W. Hoogland (CERN Report No. 87-08, Geneva, 1987), Vol. 2, p. 414.
²⁰J. Cortés, K. Hagiwara, and F. Herzog, Nucl. Phys. **B278**, 26 (1986); J. Stroughair and C. Bilchak, Manchester Report No. M/C TH-83/29, 1984 (unpublished).
²¹D. Duke and J. Owens, Phys. Rev. D **30**, 49 (1984).